


Cite this: *Food Funct.*, 2024, 15, 6424

# Anti-obesity effects of a standardized ethanol extract of *Eisenia bicyclis* by regulating the AMPK signaling pathway in 3T3-L1 cells and HFD-induced mice†

Young-Seo Yoon,<sup>a,b</sup> Kyung-Sook Chung,<sup>a</sup> Su-Yeon Lee,<sup>a</sup> So-Won Heo,<sup>a,b</sup> Ye-Rin Kim,<sup>a,c</sup> Jong Kil Lee,<sup>c,d</sup> Hyunjae Kim,<sup>e</sup> Soyoon Park,<sup>e</sup> Yu-Kyong Shin<sup>e</sup> and Kyung-Tae Lee  <sup>\*a,b,c</sup>

Obesity requires treatment to mitigate the potential development of further metabolic disorders, including diabetes, hyperlipidemia, tumor growth, and non-alcoholic fatty liver disease. We investigated the anti-obesity effect of a 30% ethanol extract of *Eisenia bicyclis* (Kjellman) Setchell (EEB) on 3T3-L1 preadipocytes and high-fat diet (HFD)-induced obese C57BL/6 mice. Adipogenesis transcription factors including peroxisome proliferator-activated receptor (PPAR) $\gamma$ , CCAAT/enhancer-binding protein-alpha (C/EBP $\alpha$ ), and sterol regulatory element-binding protein-1 (SREBP-1) were ameliorated through the AMP-activated protein kinase (AMPK) pathway by EEB treatment in differentiated 3T3-L1 cells. EEB attenuated mitotic clonal expansion by upregulating cyclin-dependent kinase inhibitors (CDKIs) while downregulating cyclins and CDKs. In HFD-fed mice, EEB significantly decreased the total body weight, fat tissue weight, and fat in the tissue. The protein expression of PPAR $\gamma$ , C/EBP $\alpha$ , and SREBP-1 was increased in the subcutaneous fat and liver tissues, while EEB decreased the expression levels of these transcription factors. EEB also inhibited lipogenesis by downregulating acetyl-CoA carboxylase (ACC) and fatty acid synthase (FAS) expression in the subcutaneous fat and liver tissues. Moreover, the phosphorylation of AMPK and ACC was downregulated in the HFD-induced mouse group, whereas the administration of EEB improved AMPK and ACC phosphorylation; thus, EEB treatment may be related to the AMPK pathway. Histological analysis showed that EEB reduced the adipocyte size and fat accumulation in subcutaneous fat and liver tissues, respectively. EEB promotes thermogenesis in brown adipose tissue and improves insulin and leptin levels and blood lipid profiles. Our results suggest that EEB could be used as a potential agent to prevent obesity.

Received 4th March 2024,  
Accepted 7th May 2024

DOI: 10.1039/d4fo00759j

rsc.li/food-function

## 1. Introduction

According to the World Health Organization (WHO), the estimates for the global levels of overweight and obesity (BMI  $\geq 25$  kg m<sup>-2</sup>) suggest an increase from 38% of the world's

population in 2020 to over 50% by 2035.<sup>1</sup> Being overweight or obese has become a prominent risk factor,<sup>2</sup> especially since COVID-19. Since obesity has consequences beyond its impact on physical appearance, it is now acknowledged as a medical condition requiring treatment to reduce the risk of developing additional metabolic disorders such as diabetes, hyperlipidemia, tumor growth, and non-alcoholic fatty liver disease.<sup>3–6</sup>

Obesity is characterized by an increase in the amount of adipose tissue, which is categorized into white adipose tissue (WAT) and brown adipose tissue (BAT).<sup>7,8</sup> WAT enlarges through an augmented adipocyte size and/or number, a process known as adipogenesis.<sup>9</sup> The AMP-activated protein kinase (AMPK) signaling pathway serves as the principal regulator of adipogenesis by maintaining cellular energy balance and physiological metabolism.<sup>10</sup> It has been confirmed that the activation of AMPK signaling downregulates transcription factors such as peroxisome proliferator-activated receptor (PPAR) $\gamma$ , CCAAT/enhancer-binding protein-alpha (C/EBP $\alpha$ ),

<sup>a</sup>Department of Pharmaceutical Biochemistry, College of Pharmacy, Kyung Hee University, Seoul, 02447, Republic of Korea. E-mail: ktlee@khu.ac.kr; Fax: +82 2 961 9580; Tel: +82 2 961 0860

<sup>b</sup>Department of Biomedical and Pharmaceutical Sciences, Graduate School, Kyung Hee University, Seoul 02447, Republic of Korea

<sup>c</sup>Department of Fundamental Pharmaceutical Science, Graduate School, Kyung Hee University, Seoul 02447, Republic of Korea

<sup>d</sup>Department of Pharmacy, College of Pharmacy, Kyung Hee University, 26 Kyungheedaero, Dongdaemun-gu, Seoul, 02447, Republic of Korea

<sup>e</sup>Department of New Material Development, COSMAXBIO, Gyeonggi, 13486, Republic of Korea

† Electronic supplementary information (ESI) available. See DOI: <https://doi.org/10.1039/d4fo00759j>



and sterol regulatory element-binding protein-1 (SREBP-1).<sup>11</sup> PPAR $\gamma$  and C/EBP $\alpha$ , upon activation, upregulate numerous genes integral to the adipocyte phenotype, including glycerophosphate dehydrogenase, insulin receptors, and fatty acid-binding proteins.<sup>12</sup> SREBP also promotes adipogenesis and sustains lipogenesis by regulating downstream lipogenic enzymes, including fatty acid synthase (FAS) and acetyl-CoA carboxylase (ACC).<sup>13–15</sup> BAT dissipates substantial amounts of chemical energy *via* uncoupled respiration and heat generation (thermogenesis).<sup>16</sup> Sirtuin 1 (SirT1) is responsible for the activation of thermogenesis by regulating WAT browning.<sup>17,18</sup> Furthermore, SirT1 has been observed to stimulate mitochondrial biogenesis by activating peroxisome proliferator-activated receptor gamma co-activator (PGC-1 $\alpha$ ).<sup>19</sup> PGC-1 $\alpha$  activates PPAR $\alpha$  and triggers the upsurged expression of uncoupling protein 1 (UCP1) and cytochrome c oxidase IV (COX IV).<sup>20,21</sup> UCP1 facilitates thermogenesis and heat generation by consuming proton gradient energy from the electron transport chain during mitochondrial respiration.<sup>22,23</sup> In addition, COX IV participates in ATP synthesis and initiates energy metabolism in the mitochondria.<sup>24</sup> Because numerous weight-loss drugs have been removed from the market owing to their severe side effects,<sup>25</sup> natural products containing various components with multiple medicinal properties are continuously explored to develop novel drugs.<sup>26</sup>

The marine environment is a unique reservoir of novel bioactive natural products, characterized by structural and chemical attributes that are typically absent in terrestrial natural products. Marine organisms are a rich source of nutraceuticals and are promising candidates for the treatment of several human diseases.<sup>27</sup> Notably, there is growing interest in utilizing bioactive compounds sourced from marine macroalgae as natural components in a wide range of nutraceuticals and dietary supplements.<sup>28</sup> Marine macroalgae are classified into green algae, brown algae, and red algae based on their pigmentation, nutritional content, and chemical composition.<sup>29</sup> *Eisenia bicyclis* (Kjellman) Setchell (*E. bicyclis*) is a prevalent brown alga hailing from the Laminariaceae family, typically found along the central Pacific coastline encompassing regions like Korea, Japan, and China. The anti-diabetic, anti-thrombotic, anti-inflammatory, and neuroprotective activities of *E. bicyclis* have been previously explored.<sup>30–34</sup> A standardized 30% ethanol extract of *E. bicyclis* (EEB) and its active constituent, dieckol, have been reported to exert anti-photoaging effects by suppressing wrinkle formation and dehydration in UVB-irradiated Hs68 cells and hairless mice.<sup>30,35</sup> Therefore, as part of our ongoing screening program to evaluate the anti-obesity potential of natural products, we investigated the efficacy and molecular mechanisms underlying the anti-obesity properties of EEB in 3T3 adipocytes and high-fat diet (HFD)-induced obesity mice.

## 2. Materials and methods

### 2.1. Chemical reagents

Standardized EEB was prepared as previously described.<sup>30</sup> In brief, the aerial parts of *E. bicyclis* were extracted with 30%

ethanol at 60–80 °C for 5 h followed by evaporation and sterilization, affording a dried extract residue EEB with a yield of 33.4% (w/w), which contained several compounds including 60.3  $\pm$  0.05  $\mu\text{g g}^{-1}$  of dieckol as the bioactive compound.<sup>30</sup> Dulbecco's modified eagle's medium (DMEM), fetal bovine serum (FBS), bovine serum (BS), penicillin–streptomycin (PS), phosphate-buffered saline (PBS), and 3-(4,5-dimethylthiazol-2-yl)-2,5-diphenyl tetrazolium bromide (MTT; L11939, Alfa Aesar) were obtained from Life Technologies Inc. (Grand Island, NY, USA). 3-Isobutyl-1-methylxanthine (IBMX, I5879), dexamethasone (D8893), insulin (I0516), Oil Red O (O0625), isopropanol (I9516), and orlistat (O4139) were purchased from Sigma-Aldrich (St Louis, MO, USA). C/EBP $\alpha$  (8178), phospho-AMPK $\alpha$  (2531), AMPK $\alpha$  (2532), PPAR $\gamma$  (2435), FABP4 (2120), phospho-ACC (3661), ACC (3662), SirT1 (9475), COX IV (4844), and p27 (2552) antibodies were purchased from Cell Signaling Technology (Danvers, MA, USA). FAS (sc-55580), PGC-1 $\alpha$  (sc-518025), PPAR $\alpha$  (sc-398394), UCP-1 (sc-293418), p21 (sc-817), cyclin D1 (sc-8396), CDK4 (sc-260), CDK6 (sc-7961), cyclin E (sc-377100), cyclin A (sc-239), CDK2 (sc-163), cyclin B1 (sc-245), CDK1 (sc-54),  $\alpha$ -tubulin (sc-5286) and  $\beta$ -actin (sc-81178) antibodies were obtained from Santa Cruz Biotechnology (Santa Cruz, CA, USA). The SREBP-1 (ab28481) antibody was purchased from Abcam (Cambridge, MA, USA). The enzyme-linked immunosorbent assay (ELISA) kits for leptin (19MALEP019) and insulin (19MAUMI518) were obtained from Morinaga (Morinaga Institute of Biological Science, Inc., Yokohama, Japan).

### 2.2. Cell culture and cell viability

3T3-L1 cells were obtained from the American Type Culture Collection (ATCC, Manassas, VA, USA). These cells were cultured in a growth medium (GM) containing 10% bovine serum and 1% penicillin–streptomycin, and seeded in 96-well plates at a density of  $2 \times 10^5 \text{ mL}^{-1}$ . After 24 h of incubation, the cells were treated with EEB at concentrations of 3.125, 6.25, 12.5, 25, 50, 100, 200, or 400  $\mu\text{g mL}^{-1}$ . After incubation for 24 h, MTT solution (5  $\text{mg mL}^{-1}$ ) was added to each well and then incubated for 2 h. The supernatant was removed and the remaining formazan was dissolved in DMSO. The absorbance was determined using a microplate reader (Molecular Devices Inc., San Jose, CA, USA) at 540 nm.

### 2.3. Adipocyte differentiation and Oil Red O staining

The differentiation and Oil Red O staining were conducted according to our previous report.<sup>36</sup> During the procedure, the 3T3-L cells were treated with or without EEB (50, 100, or 200  $\mu\text{g mL}^{-1}$ ).

### 2.4. Western blot analysis

Proteins were extracted from differentiated 3T3-L1 cells, subcutaneous fat tissue, liver tissue, and brown adipose tissue as previously described.<sup>37</sup> The extracted proteins were quantified using the Bradford assay. The whole proteins (30  $\mu\text{g}$ ) were separated by SDS-PAGE using 8–15% acrylamide gel and then transferred to a PVDF membrane. The blots were incubated with primary antibodies diluted in 2.5% skim milk with a



1 : 1000 ratio. After incubation for 18 h at 4 °C, the blots were washed with TBS/T three times and incubated with secondary antibodies diluted in 5% skim milk with a 1 : 2000 ratio for 2 h at 25 °C. The blots were then washed three times with TBS/T, and developed using an ECL chemiluminescence substrate (Santa Cruz Biotechnology, Santa Cruz, CA, USA). For the visualization of the developed blots, the Amersham Hyperfilm ECL (GE Healthcare Life Sciences, Chicago, IL, USA) was used.

### 2.5. Propidium iodide (PI) staining

The PI staining was performed according to our previous report.<sup>11</sup> PI stained cells were then analyzed by flow cytometry (Cytomics FC 500, Beckman Coulter Inc., Brea, CA, USA).

### 2.6. HFD-induced obesity animal models

Male C57BL/6J mice (6 weeks, weight 20 g ± 10%) were obtained from Orient Bio Inc. (Seongnam, Korea). The animals were subjected to standardized conditions (light/dark cycle, 12 h; temperature, 20 ± 2 °C; humidity, 50 ± 10%) with free access to food and water. After the acclimation of mice for 1 week, they were separated into 5 groups: control group, HFD-induced obesity group, orlistat group, and EEB (100 or 300 mg kg<sup>-1</sup>) group. The control group was fed a normal diet while the other groups were fed 30% HFD for 13 weeks. Table 1 shows the ingredient composition for normal diet and high-fat diet. Along with the diet supplement, the control and HFD-induced groups were orally administered with the vehicle, and the orlistat and EEB groups were orally administered with 10 mg kg<sup>-1</sup> of orlistat and 100 or 300 mg kg<sup>-1</sup> of EEB. The oral administration and body weight measurement were performed daily and every week, respectively. At the end of the experiment, sacrifice was conducted for obtaining subcutaneous fat, gonadal fat, mesenteric fat, renal fat, brown fat, and liver. The obtained tissues were immediately frozen in liquid nitrogen. All animal experiments adhered to the University Guideline of the Ethical Committee for Animal Care and the Use of Laboratory Animals, College of Pharmacy, Kyung Hee University, in accordance with an animal protocol (KHSASP-22-197).

### 2.7. Body fat composition

The body fat composition of each group was determined by the total body scanning method, dual-energy X-ray absorptiometry (DXA) (InAlyzer, Medikors, Seongnam, Korea). The blue color, yellow/green color, and red color represent lean tissue, differentiated tissue from lean to fat, and fat tissue, respectively.

**Table 1** Ingredient composition of a normal and high-fat diet

Comparative profiles	Normal diet (%)	High fat diet (%)
Protein	18	13
Fat	5.2	30
Crude fiber	6.7	4
Ash	5.7	4
Moisture	4.3	3
Carbohydrate	55.9	41
Others	5.7	4

### 2.8. Histological analysis

Subcutaneous fat tissues and liver tissues were obtained and fixed overnight in 4% paraformaldehyde. Subcutaneous fat or liver-embedded paraffin blocks were then sliced and stained using hematoxylin and eosin. Stained slices were observed with an optical microscope (Olympus, Tokyo, Japan).

### 2.9. Plasma parameters

Blood samples were collected from the veins of anesthetized mice using a 10 U mL<sup>-1</sup> heparin sodium-coated syringe. The preparation and biochemical examination of plasma parameters were implemented by following the guidelines of T&P Bio Co. (Gwangju, Republic of Korea).

### 2.10. Statistical analysis

The values are expressed as the mean ± SD or SEM of *in vitro* or *in vivo* experiments, respectively. Statistically significant values were compared using ANOVA and Dunnett's *post-hoc* test, and *P*-values of less than 0.05 were considered statistically significant.

## 3. Results

### 3.1. EEB prevents 3T3-L1 cells from differentiating into adipocytes

First, to establish appropriate experimental concentrations in a cell-based system, the effect of EEB on cell viability was determined using the MTT assay. As the treatment of EEB did not affect cell viability up to 400 µg mL<sup>-1</sup>, the experiment was conducted at concentrations of 50, 100, or 200 µg mL<sup>-1</sup> (Fig. 1A). To examine the inhibitory effects of EEB on intracellular lipid accumulation, Oil Red O staining was performed. The differentiation of 3T3-L1 cells resulted in lipid accumulation, whereas treatment with EEB diminished this accumulation in a concentration-dependent manner (Fig. 1B and C). EEB effectively inhibited lipid accumulation and the related proteins were identified. As shown in Fig. 1D, EEB treatment upregulated the differentiation medium (DM)-induced reduced p-AMPK expression. Moreover, EEB significantly lowered the levels of adipogenesis-related proteins including FABP4, PPARγ, C/EBPα, and mature SREBP-1, and restored the level of the precursor of SREBP-1.

### 3.2. EEB attenuates mitotic clonal expansion in differentiated 3T3-L1 cells

Adipocyte differentiation involves a process called mitotic clonal expansion (MCE), which occurs during the initial phase of adipogenesis.<sup>38</sup> We hypothesized that EEB would attenuate MCE and measured the cell cycle by performing PI staining. By the differentiation of 3T3-L1 cells following DM treatment, a decrease in the G<sub>1</sub> phase ratio (69.8–31.3%) and a simultaneous increase in the G<sub>2</sub>/M phase ratio (19.4–59.2%) were observed. Meanwhile, EEB at 200 µg mL<sup>-1</sup> restored these altered ratios (G<sub>1</sub> phase ratio: from 31.3–38.0% and G<sub>2</sub>/M phase ratio: 59.2–51.2%). These data indicated that the cell cycle was



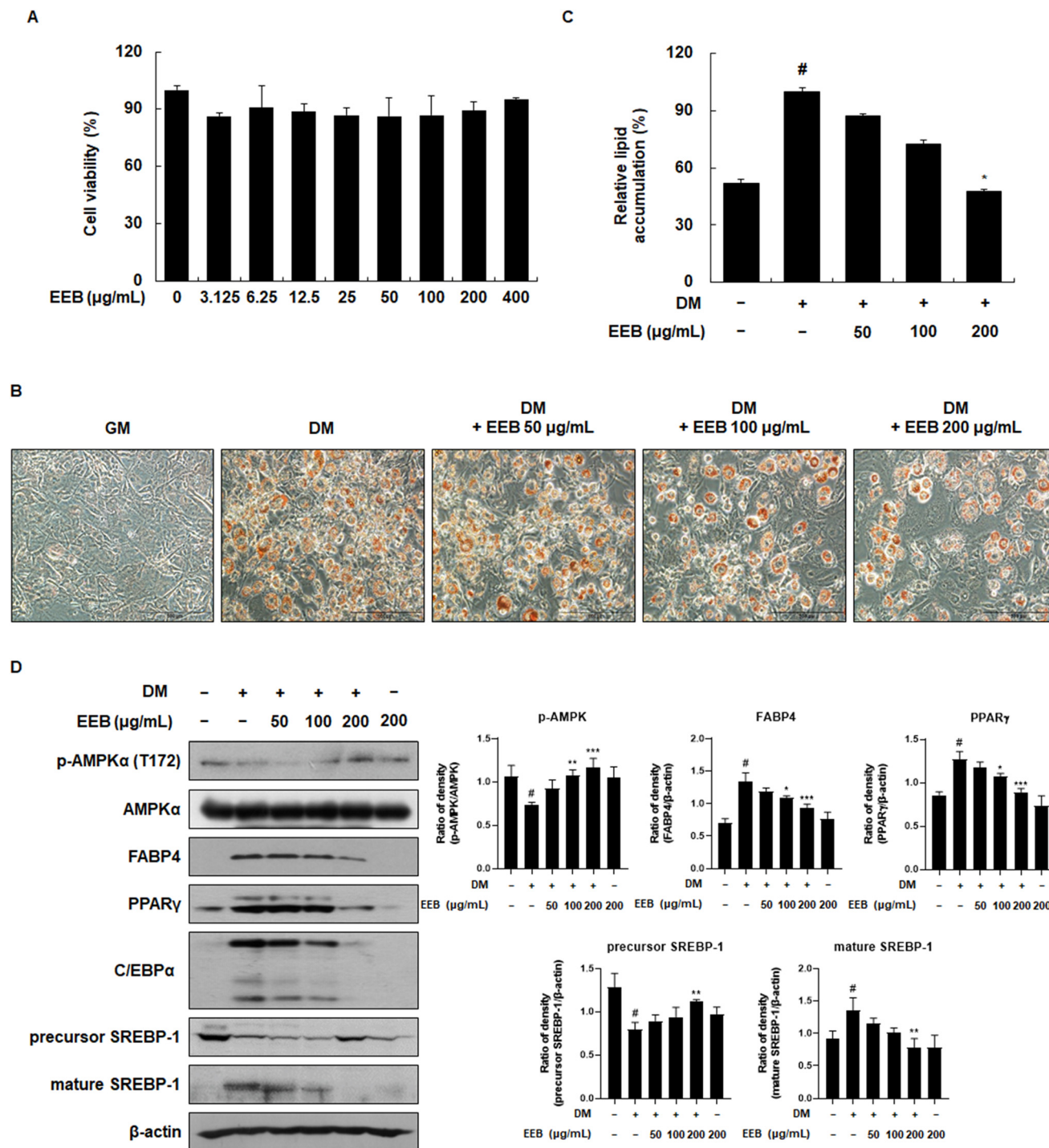


**Fig. 1** Effects of treatment of EEB on differentiated 3T3-L1 cells. 3T3 cells were differentiated with or without treatment of EEB (50–200 µg mL<sup>-1</sup>). (A) Cell viability was measured using an MTT assay under growth medium conditions. (B) The cells were fixed and stained with Oil Red O. Representative microscopy images of stained cells (200× magnification). (C) The stained lipid droplets were dissolved in isopropanol and the quantification of intracellular lipid accumulation was performed. (D) The expression of adipocyte differentiation-related proteins was estimated by western blotting using specific protein antibodies. β-Actin protein was used as an internal control. Densitometric analysis was performed using Bio-Rad Quantity One software (BioRad; Hercules, CA, USA). Values are expressed as means ± SD. #*p* < 0.05 vs. the GM control group; \**p* < 0.05, \*\**p* < 0.01, and \*\*\**p* < 0.001 as compared to the DM control group.

triggered by DM treatment, whereas EEB treatment mildly released these cell cycle arrests (Fig. 2A). Furthermore, we analyzed the effects of EEB on cell cycle-related proteins in 3T3-L1

cells. As shown in Fig. 2B, EEB treatment dose dependently increased the protein levels of CDK inhibitors, including p21 and p27, which were reduced by DM treatment. Based on



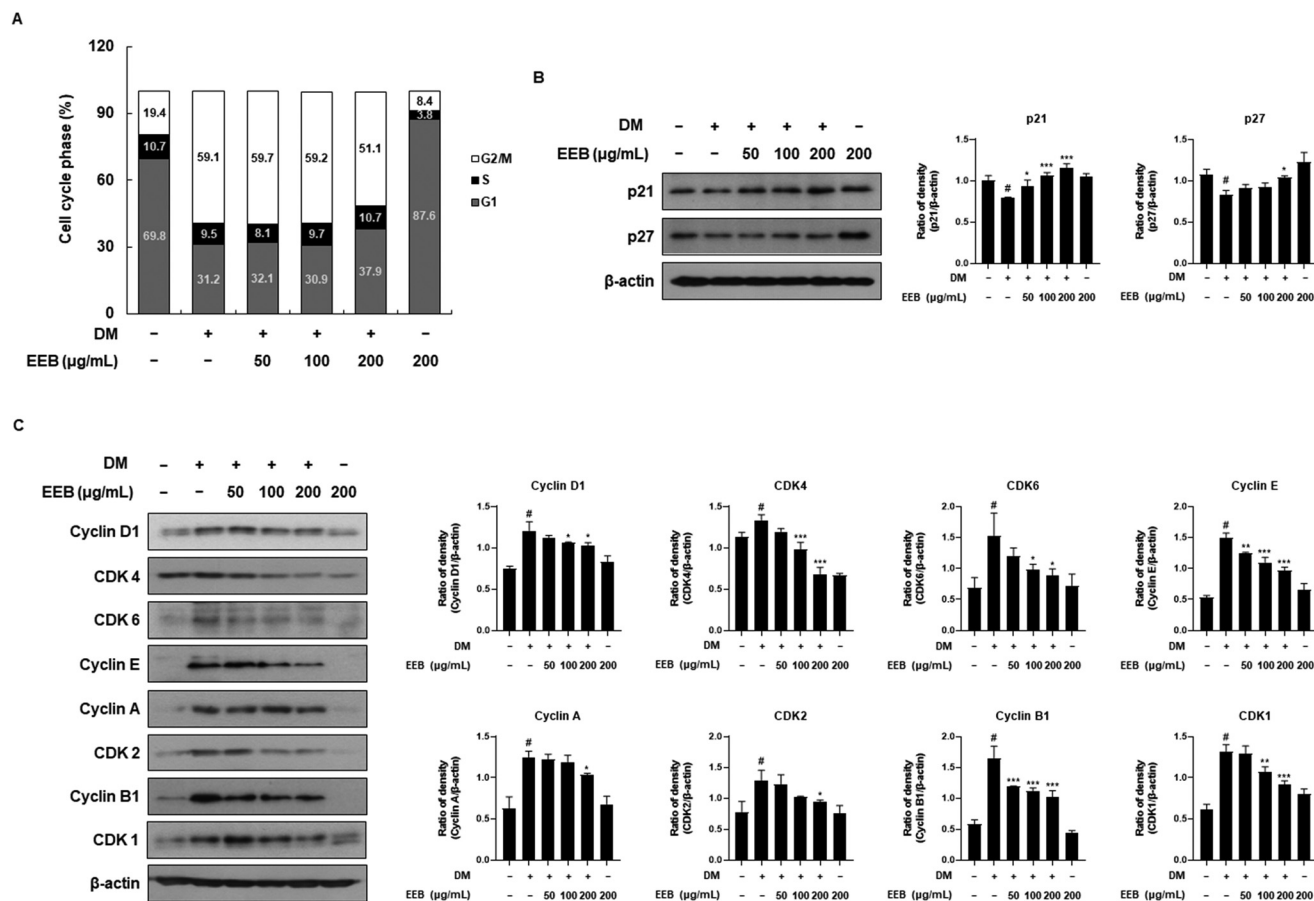


**Fig. 2** Effects of treatment of EEB on mitotic clonal expansion in differentiated 3T3-L1 cells. 3T3 cells were differentiated with or without treatment of EEB (50–200  $\mu\text{g mL}^{-1}$ ). (A) The cell cycle ratio was estimated by flow cytometry. (B and C) The expression of cell cycle-related proteins was estimated by western blotting using specific protein antibodies.  $\beta$ -Actin protein was used as an internal control. Densitometric analysis was performed using Bio-Rad Quantity One software (BioRad; Hercules, CA, USA). Values are expressed as means  $\pm$  SD. # $p < 0.05$  vs. the GM control group; \* $p < 0.05$ , \*\* $p < 0.01$ , and \*\*\* $p < 0.001$  as compared to the DM control group.

these data, EEB significantly downregulated cyclins, including cyclins D1, E, A, and B1, and CDKs, including CDK4, CDK6, CDK2, and CDK1 (Fig. 2C).

### 3.3. EEB lowers body weight gain and fat in tissue in HFD-induced C57BL/6 mice

Based on our *in vitro* data, an *in vivo* experiment was performed using an HFD-induced obese mouse model to determine the anti-obesity effects of EEB. During the 13 weeks of the experiment, significant body weight gain was observed in the HFD group compared to the normal diet control group, while the oral administration of EEB (100  $\text{mg kg}^{-1}$  or 300  $\text{mg kg}^{-1}$ ) effectively lowered body weight acquisition from 4 weeks (Fig. 3A). As shown in Fig. 3B, the HFD group exhibited a marked increase in the final body weight at the end of the experiment compared to the control group, and EEB administration significantly reduced body weight in a dose-dependent manner compared to the HFD group. In addition, gonad, mesentery, and renal fat weights were increased by the HFD; however, EEB significantly reduced the fat weight of each

organ (Fig. 3C–E). Using the DXA analysis, the body fat composition in each group was graphically optimized. The body fat accumulated in the HFD group; in contrast, it was significantly reduced in the EEB (100 and 300  $\text{mg kg}^{-1}$ )-treated groups (Fig. 3F and G).

### 3.4. EEB diminishes adipogenesis and lipogenesis through the AMPK signalling pathway in subcutaneous fat and liver tissue of HFD-induced C57BL/6 mice

Subcutaneous fat is considered a parameter for determining obesity<sup>39</sup> and an elevated risk of developing non-alcoholic fatty liver disease (NAFLD).<sup>40</sup> Therefore, we further investigated the anti-obesity effects of EEB on subcutaneous fat and liver tissues of HFD-induced C57BL/6 mice. Despite the HFD increase in subcutaneous fat and liver weight, EEB administration significantly decreased the subcutaneous fat and liver weight (Fig. 4A and 5A). Immunoblotting was performed to clarify these effects. Consistent with the *in vitro* data, EEB administration upregulated HFD-induced AMPK activation in both the subcutaneous fat and liver tissue in a



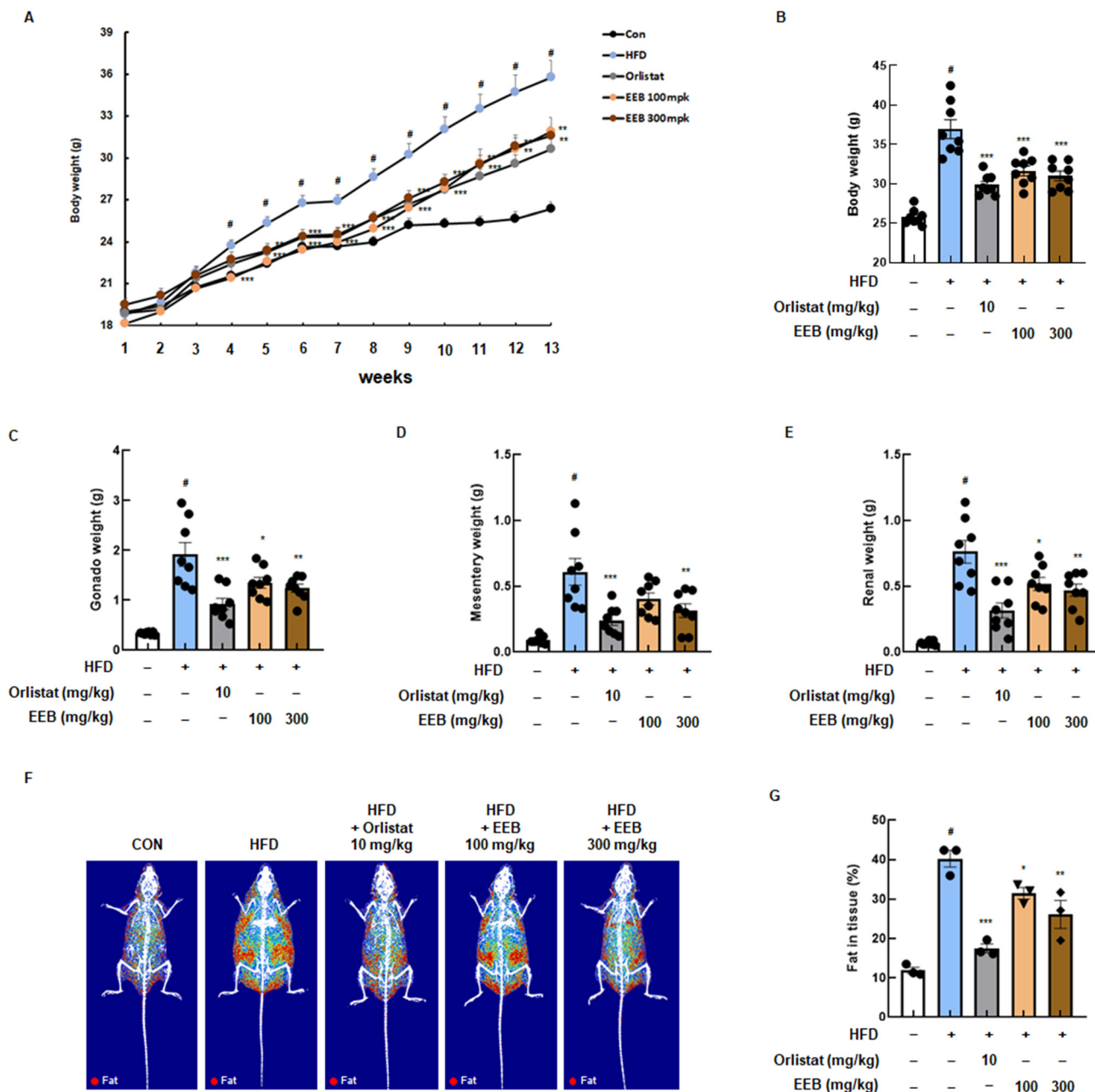


**Fig. 3** Effects of oral administration of EEB on body weight gain and fat in tissue in HFD-induced C57BL/6J mice. HFD-induced C57BL/6J mice were administered with EEB (100 or 300 mg kg<sup>-1</sup>) 5 times a week for 13 weeks. (A) Body weight was measured from week to week and (B) the final body weight changes. The subcutaneous fat weight of the (C) gonad, (D) mesentery, and (E) renal was measured. (F and G) The composition image of body fat and the value of fat in tissue were confirmed using dual X-ray absorptiometry. Values are expressed as means  $\pm$  SEM (body weight change group;  $n = 8$ , DXA group;  $n = 3$ ). # $p < 0.05$  vs. the normal diet-fed control group; \* $p < 0.05$ , \*\* $p < 0.01$ , and \*\*\* $p < 0.001$  as compared to the HFD-induced group.

dose-dependent manner (Fig. 4B and 5B). The upregulated protein expression of adipogenesis-related transcription factors including PPAR $\gamma$ , C/EBP $\alpha$ , and SREBP-1 by HFD was considerably improved by EEB administration (Fig. 4C and 5C). In addition, the HFD downregulated the ratio of p-ACC/ACC and the protein expression of FAS, whereas the administration of EEB ameliorated these effects, indicating the inhibition of fatty acid synthesis (Fig. 4D and 5D).

### 3.5. EEB reduces the size of adipocytes in subcutaneous tissue and lipid accumulation in the liver tissue of HFD-induced C57BL/6 mice

To investigate the histological effects of EEB on the subcutaneous and liver tissues in HFD-induced obese mice, H&E staining was performed. In the subcutaneous tissue, the diameter of the adipocytes in the HFD group was higher than that in the control group. However, the administration of EEB sig-



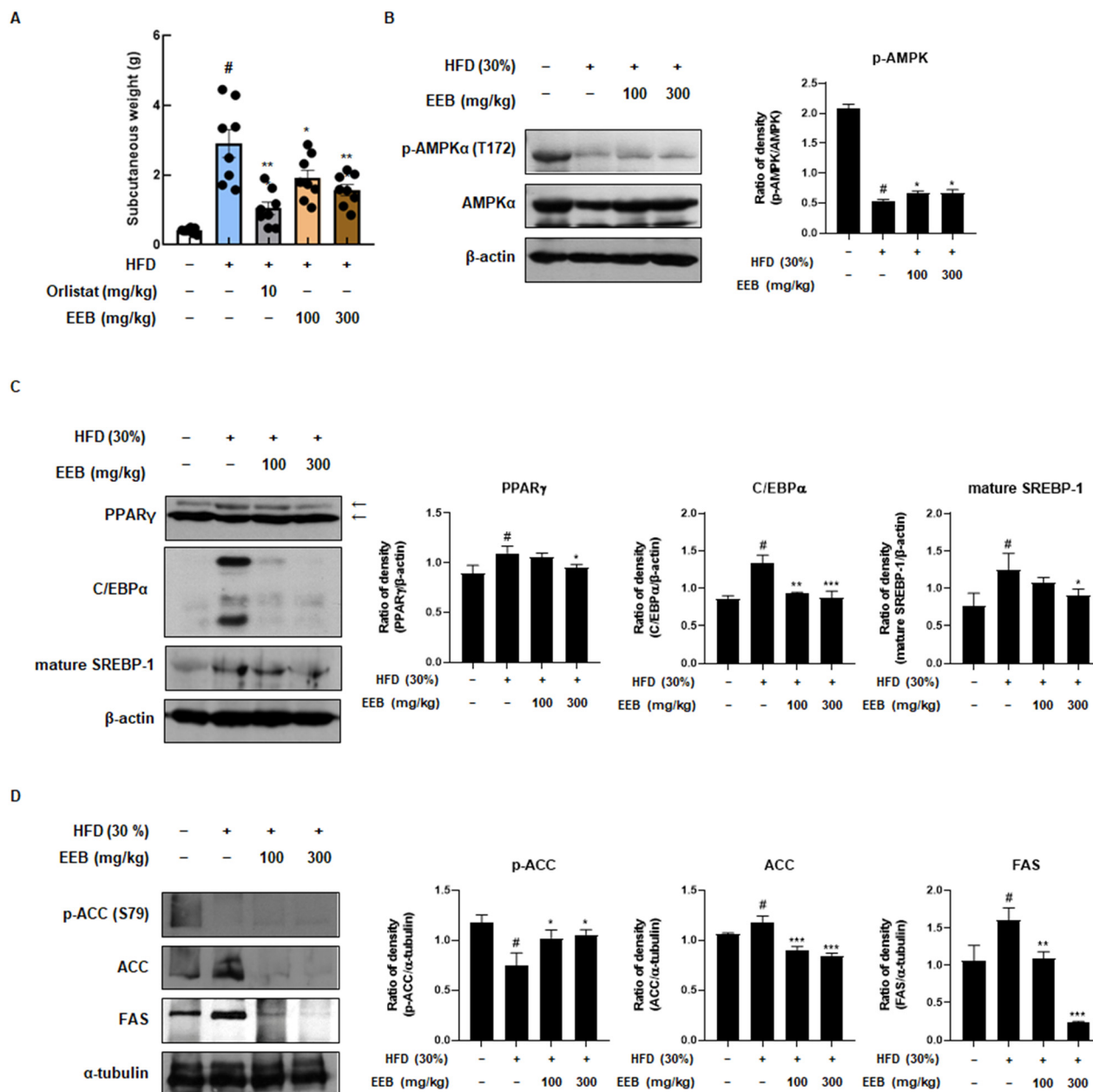


**Fig. 4** Effects of oral administration of EEB on the subcutaneous fat of HFD-induced C57BL/6J mice. (A) The weight of subcutaneous fat was measured. The expressions of (B) p-AMPK $\alpha$ , (C) adipogenesis-related proteins and (D) lipogenesis-related proteins were estimated by western blotting using specific protein antibodies.  $\beta$ -Actin protein was used as an internal control. Densitometric analysis was performed using Bio-Rad Quantity One software (BioRad; Hercules, CA, USA). Values are expressed as means  $\pm$  SEM (subcutaneous fat;  $n = 8$ , density;  $n = 3$ ). <sup>#</sup> $p < 0.05$  vs. the normal diet-fed control group; \* $p < 0.05$ , \*\* $p < 0.01$ , and \*\*\* $p < 0.001$  as compared to the HFD-induced group.

nificantly downsized the enlarged adipocytes in a concentration-dependent manner (Fig. 6A). A histological analysis of liver tissue revealed that EEB administration significantly reduced HFD-induced lipid accumulation (Fig. 6B).

### 3.6. EEB promotes thermogenesis in the BAT of HFD-induced C57BL/6 mice

BAT is linked to energy expenditure owing to its abundant mitochondria and its role in generating heat through

uncoupled respiration, a process known as thermogenesis.<sup>24</sup> Although the weight of BAT was not significantly influenced in the HFD group, it was confirmed that the BAT weight was increased by EEB oral administration (Fig. 7A). We then investigated the expression levels of thermogenesis-related factors such as SirT1, PGC-1 $\alpha$ , PPAR $\alpha$ , and UCP-1. EEB significantly reversed these reductions in HFD-fed mice. In addition, although the protein level of COX IV, which contributes to the production of ATP, was downregulated by HFD, EEB adminis-



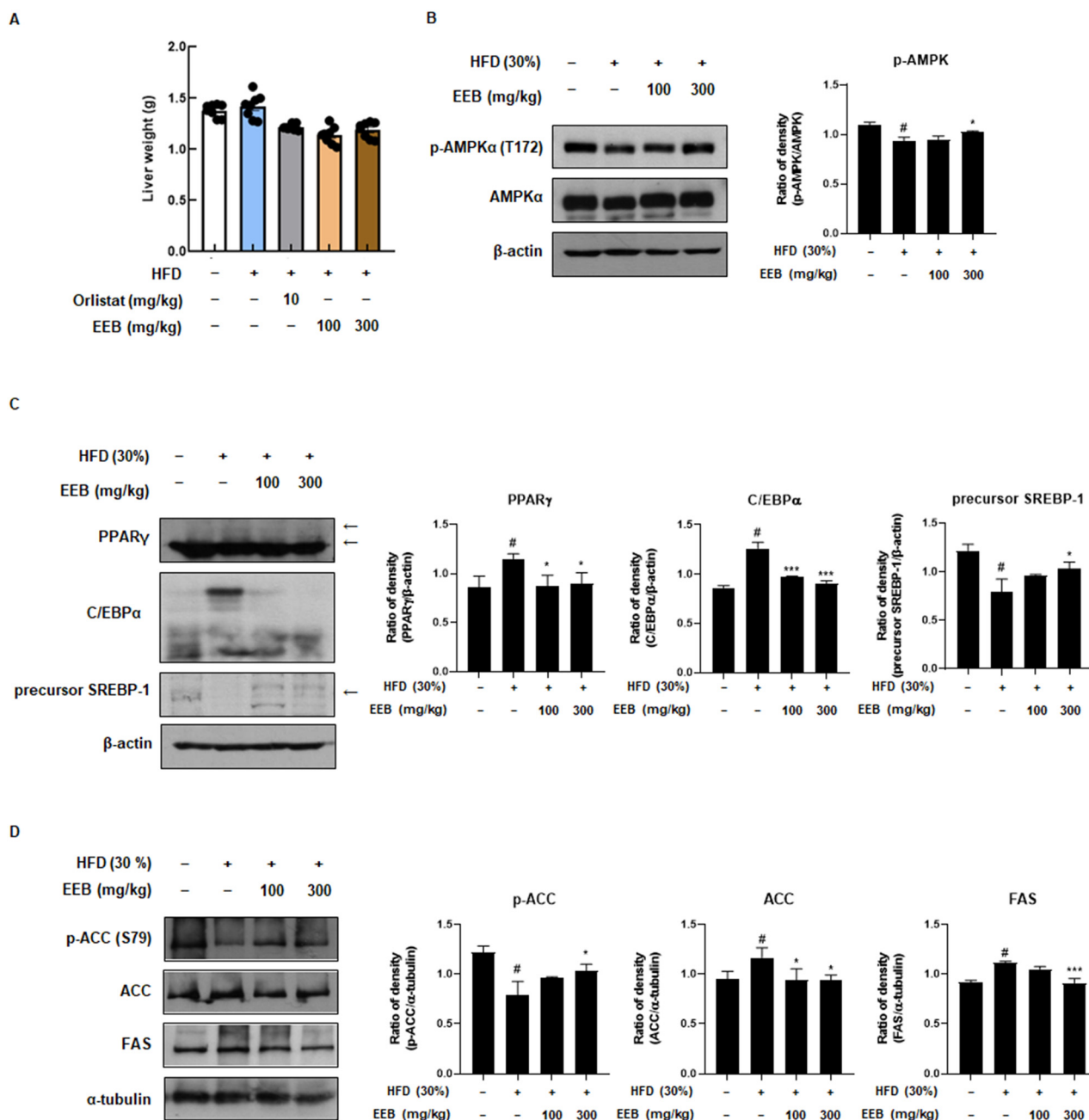


**Fig. 5** Effects of oral administration of EEB on the liver tissue of HFD-induced C57BL/6J mice. (A) The weight of liver tissue was measured. The expressions of (B) p-AMPK $\alpha$ , (C) adipogenesis-related proteins and (D) lipogenesis-related proteins were estimated by western blotting using specific protein antibodies.  $\beta$ -Actin protein was used as an internal control. Densitometric analysis was performed using Bio-Rad Quantity One software (BioRad; Hercules, CA, USA). Values are expressed as means  $\pm$  SEM (liver weight;  $n = 8$ ; density;  $n = 3$ ).  $^{\#}p < 0.05$  vs. the normal diet-fed control group;  $*p < 0.05$  and  $***p < 0.001$  as compared to the HFD-induced group.

tration considerably upregulated COX IV protein levels (Fig. 7B).

### 3.7. EEB improves the insulin and leptin levels, and lipid profile in the plasma of HFD-induced C57BL/6 mice

As HFD is known to induce dyslipidemia and cardiac pathological alterations,<sup>41</sup> we analyzed insulin and leptin levels, and lipid profiles in the plasma of each group. High levels of

insulin and leptin were observed in the plasma of the HFD group, whereas the oral administration of EEB significantly decreased plasma insulin and leptin levels (Fig. 8). As shown in Table 2, EEB significantly decreased the plasma levels of HFD-induced TC and LDL. Meanwhile, there were no considerable alterations in HDL and TG levels after EEB administration (Table 2). Furthermore, by measuring the plasma levels of GOT, GPT, and BUN in HFD-fed C57BL/6 mice, we found that





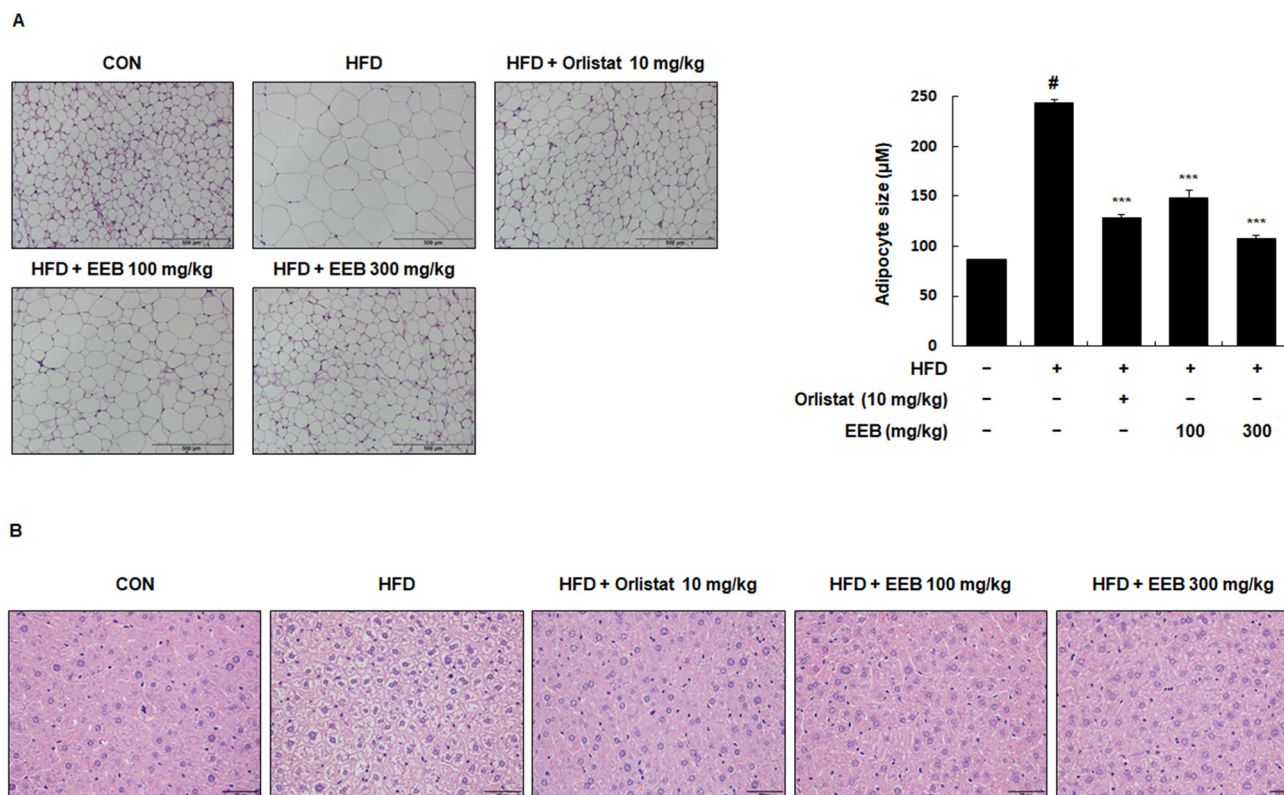


**Fig. 6** Effects of oral administration of EEB on lipid accumulation and adipocyte hypertrophy in the liver tissue and subcutaneous fat tissue of HFD-induced C57BL/6J mice, respectively. Liver tissue and subcutaneous fat tissue were stained with hematoxylin and eosin (H&E). (A) Adipocyte hypertrophy and (B) lipid accumulation were estimated via microscopic analysis. Values are expressed as means  $\pm$  SEM ( $n = 3$ ). <sup>#</sup> $p < 0.05$  vs. the normal diet-fed control group; <sup>\*\*\*</sup> $p < 0.001$  as compared to the HFD-induced group.

EEB did not cause hepatotoxicity or nephrotoxicity (ESI Fig. 1†).

## 4. Discussion

Obesity is a major health problem because it causes metabolic syndromes such as hyperlipidemia, type 2 diabetes, tumor growth, and non-alcoholic fatty liver disease.<sup>4–6</sup> Pharmacological approaches aimed at weight reduction can be advantageous in addressing obesity and decreasing the likelihood of obesity-related health conditions. Nonetheless, numerous weight-loss drugs have been removed from the market owing to their severe side effects.<sup>25</sup> Along with increased efficacy and a lower incidence of side effects, natural products have been suggested to possess the potential to expedite the development of enhanced obesity management strategies.<sup>3</sup> Natural products contain various components with multiple medicinal properties.<sup>42</sup> Accordingly, our previous study reported that the natural products of water extracts from the leaves of *Hydrangea serrata* (Thunb.) Ser, a botanical mixture of 30% ethanol extract from the leaves of *Inula japonica* and *Potentilla chinensis*, and a 30% ethanol extract of *Cassia mimosoides* var. *Makino* have been shown to possess

anti-obesity effects.<sup>36,43</sup> In particular, we have reported the anti-photoaging effects of EEB via the MAPK/AP-1, Smad, and ROS-mediated Nrf2 pathways.<sup>30</sup> Since the anti-obesity effects of *E. bicyclis* have not been revealed to date, in this study, we evaluated the anti-obesity efficacy and revealed the molecular mechanism of EEB in differentiated 3T3-L1 preadipocytes and an HFD-induced C57BL/6 mouse model.

Obesity is associated with adipocyte differentiation and maturation.<sup>44</sup> Since adipocyte differentiation is accompanied by adipogenesis, lipogenesis, and cell cycle regulation,<sup>45</sup> we focused on these signaling pathways to elucidate the anti-obesity effects of EEB. PPAR $\gamma$  and C/EBP $\alpha$  play a key role in the complex transcriptional cascade during adipocyte differentiation.<sup>46</sup> They reciprocally stimulate each other's expression and cooperate to activate many metabolic adipocyte genes.<sup>47</sup> SREBP also plays a role in controlling the equilibrium between intracellular fat levels and lipogenesis.<sup>48</sup> SREBP-1c is a transcription factor that is synthesized as a precursor in the membranes of the endoplasmic reticulum and requires post-translational modification to yield its transcriptionally active nuclear form. When activated, it transitions from the membrane to the nucleus as a mature protein, which is the only form that can function as a transcription factor.<sup>15,49</sup> It is presumed that SREBP regulates the coordinated transcriptional



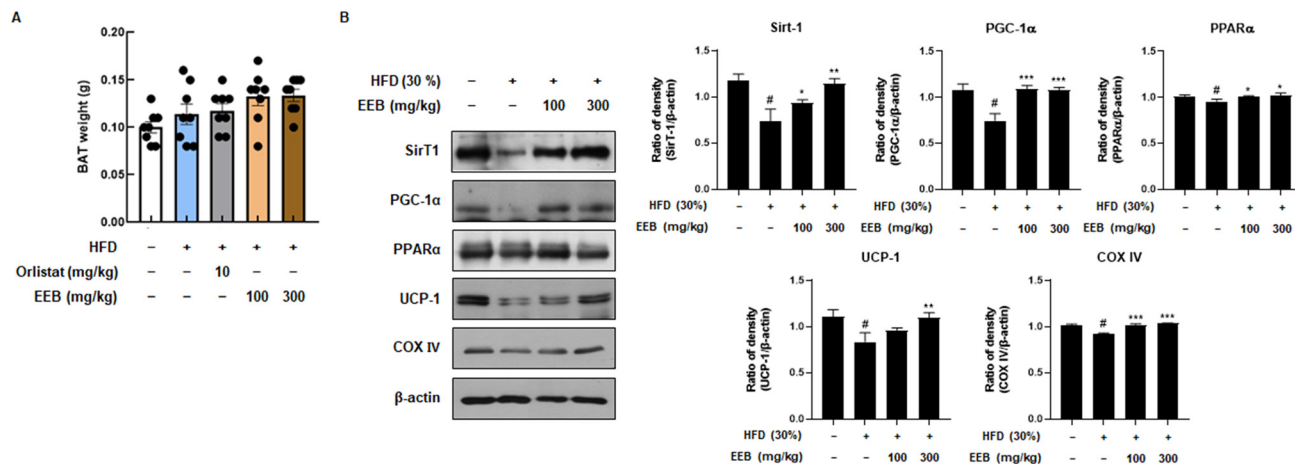


**Fig. 7** Effects of oral administration of EEB on the brown adipose tissue of HFD-induced C57BL/6J mice. (A) The weight of brown adipose tissue was measured. (B) The expression of thermogenesis-related proteins was estimated by western blotting using specific protein antibodies.  $\beta$ -Actin protein was used as an internal control. Densitometric analysis was performed using Bio-Rad Quantity One software (BioRad; Hercules, CA, USA). Values are expressed as means  $\pm$  SEM (brown adipose tissue;  $n = 8$ , density;  $n = 3$ ). # $p < 0.05$  vs. the normal diet-fed control group; \* $p < 0.05$ , \*\* $p < 0.01$ , and \*\*\* $p < 0.001$  as compared to the HFD-induced group.

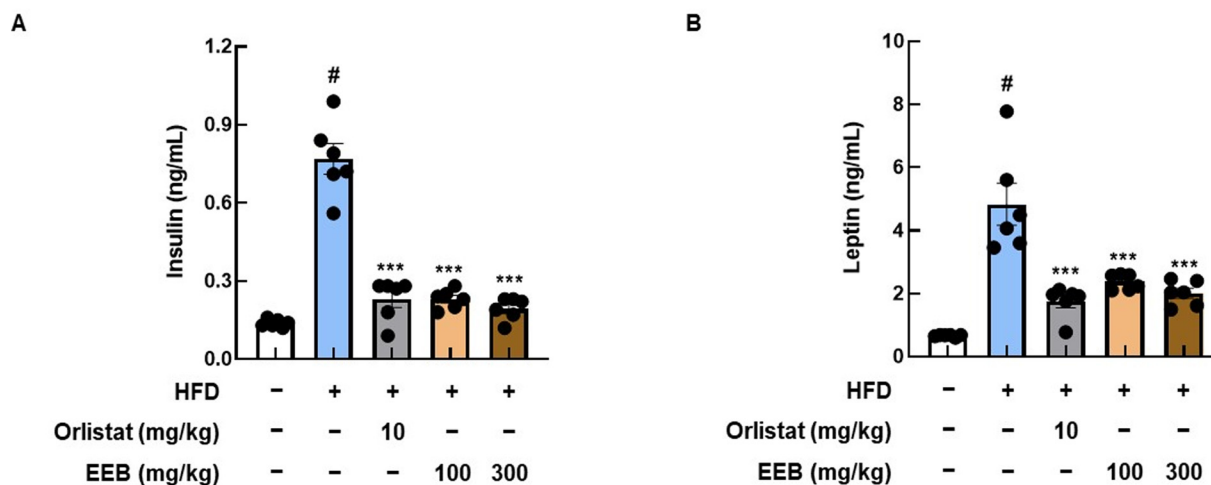


**Fig. 8** Effects of oral administration of EEB on the levels of insulin and leptin in the plasma of HFD-induced C57BL/6J mice. The levels of (A) insulin and (B) leptin in plasma were estimated using ELISA kits. Values are expressed as means  $\pm$  SEM ( $n = 6$ ). # $p < 0.05$  vs. the normal diet-fed control group; \*\*\* $p < 0.001$  as compared to the HFD-induced group.

**Table 2** Effects of oral administration of EEB on the level of blood lipid in HFD-induced C57BL/6J mice

Blood lipid (mg dl <sup>-1</sup> )	Control	HFD	Orlistat (10 mg kg <sup>-1</sup> )	EEB (100 mg kg <sup>-1</sup> )	EEB (300 mg kg <sup>-1</sup> )
TC	81.33 $\pm$ 2.35	143.83 $\pm$ 5.30 <sup>#</sup>	124.33 $\pm$ 4.67*	136.00 $\pm$ 3.61	130.33 $\pm$ 4.72
TG	50.00 $\pm$ 2.93	51.00 $\pm$ 3.58	30.67 $\pm$ 4.67*	53.17 $\pm$ 6.97	44.50 $\pm$ 4.10
HDL	68.67 $\pm$ 1.41	86.50 $\pm$ 2.26	93.33 $\pm$ 1.36	97.50 $\pm$ 5.17	92.50 $\pm$ 1.57
LDL	7.33 $\pm$ 0.21	12.00 $\pm$ 0.52 <sup>#</sup>	8.50 $\pm$ 0.34***	10.50 $\pm$ 0.22	9.17 $\pm$ 0.54***

Values are expressed as means  $\pm$  SEM ( $n = 6$ ). # $p < 0.05$  vs. the normal diet-fed control group; \* $p < 0.05$  and \*\*\* $p < 0.001$  as compared to the HFD-induced group.

regulation of FAS and ACC.<sup>50,51</sup> FAS, the main synthetic enzyme that catalyzes the condensation of malonyl-CoA to produce 16-carbon saturated fatty acid palmitate, and ACC,

which synthesizes malonyl-CoA from acetyl-CoA, are essential in the fatty acid biosynthetic pathway.<sup>15</sup> AMPK is a major cellular energy sensor and regulator of metabolic homeostasis that



modulates protein, lipid, and glucose metabolism.<sup>52</sup> The activation of AMPK, as an important upstream modulator, inhibits adipogenesis and lipogenesis by downregulating PPAR $\gamma$ , C/EBP $\alpha$ , and SREBP.<sup>53,54</sup> In this study, we determined that EEB exerted anti-obesity effects *in vitro* and *in vivo* by inhibiting adipogenesis and lipogenesis through the activation of AMPK.

Initiation of the transcriptional cascade for adipocyte differentiation is dependent on cell division and cell proliferation during MCE. The evidence of the MCE process is demonstrated by hindered proliferation, cell cycle entry into the S phase, the transition from the S to the G2/M phase in confluent cells, and alterations in the levels of cell cycle-regulating proteins, including CDKs and their regulatory cyclin subunits.<sup>55,56</sup> Furthermore, cyclin/CDKs themselves are negatively regulated by CDKIs such as p21 and p27.<sup>57</sup> Our results showed that treatment with EEB upregulated p21 and p27 and downregulated cyclin and CDK expression. These data revealed that EEB attenuates MCE by regulating cell cycle-related pathways.

Energy expenditure for thermogenesis in BAT serves either to maintain the body temperature or to dissipate excess dietary energy.<sup>58</sup> SirT1 affects the differentiation and remodeling of BAT by regulating the activity of PGC-1 $\alpha$ , a critical regulator of BAT thermogenesis, which is highly inducible by environmental stimuli such as cold and diet.<sup>59,60</sup> In addition, PGC-1 $\alpha$  is known to activate PPAR $\alpha$  and induce UCP-1 transcription in mouse brown adipose tissue.<sup>20,60</sup> Furthermore, the transcription rate of COX-IV, a major component of the inner mitochondrial membrane electron transport chain, can also be increased by PGC-1 $\alpha$  directly or indirectly.<sup>21,61</sup> In the present study, EEB administration restored the HFD-induced protein expression levels of SirT1, PGC-1 $\alpha$ , PPAR $\alpha$ , UCP-1, and COX-IV. Because these proteins are involved in BAT thermogenesis, they can be expected to contribute to energy expenditure by promoting thermogenesis.

In our previous research, we have elucidated the chemical constituents of EEB, including eckol, phloroeckol, 6,6'-bieckol, 6,8'-bieckol, 8,8'-bieckol, dieckol, and phlorofucofuroeckol A.<sup>30</sup> Among these, we speculate that eckol,<sup>62</sup> 6,6'-bieckol,<sup>63</sup> dieckol,<sup>64</sup> and phlorofucofuroeckol A,<sup>62</sup> for which anti-obesity effects have already been confirmed, along with phloroeckol, 6,8'-bieckol, and 8,8'-bieckol, for which anti-obesity effects have not yet been verified, appear to have anti-obesity effects comprehensively in EEB. Our study is mainly focused on adipogenesis and lipogenesis *in vitro* and *in vivo*. However, lipogenesis is closely related to lipid metabolism.<sup>65</sup> To elucidate a more detailed anti-obesity mechanism of EEB, it seems that further studies on lipid metabolism are necessary.

We also previously reported that the oral administration of EEB (50, 100, and 200 mg kg<sup>-1</sup>) prevents UVB-induced skin damage in a dose-dependent manner<sup>30</sup> and a significant reduction in trans-epidermal water loss, epidermal/dermal thickness, and wrinkle formation in hairless mice administered with dieckol (an active constituent of EEB, 5 and 10 mg kg<sup>-1</sup>). As this experiment was designed to expand the indication capacity of EEB, we evaluated using EEB at 100 and

300 mg kg<sup>-1</sup> dosage based on our previous experiment. Through the results of this experiment, it was found that the body fat reduction effect was saturated at 100 mg kg<sup>-1</sup> administration. Further studies are needed to obtain the optimal administration to provide anti-obesity effects.

## 5. Conclusion

In summary, our data showed that EEB treatment attenuated the proliferation, differentiation, and MCE of 3T3-L1 cells. Oral administration of EEB in HFD-fed mice downregulated adipogenesis and lipogenesis in subcutaneous and liver tissues and upregulated thermogenesis in BAT by regulating related proteins. EEB also improved adipogenic hormones and the lipid composition of HFD-induced mouse plasma. Collectively, our results suggest that EEB has the potential to prevent diet-induced obesity *via* weight loss.

## Author contributions

Conceptualization: Yu-Kyong Shin and Kyung-Tae Lee; data curation: Young-Seo Yoon; formal analysis: Young-Seo Yoon, Su-Yeon Lee, and Ye-Rin Kim; funding acquisition: Yu-Kyong Shin and Kyung-Tae Lee; investigation: Young-Seo Yoon, Su-Yeon Lee, and Ye-Rin Kim; methodology: Kyung-Sook Chung and Kyung-Tae Lee; writing – original draft preparation: Young-Seo Yoon; writing – review and editing: Kyung-Sook Chung and Kyung-Tae Lee; resources: Jong Kil Lee, Hyunjae Kim, Soyoon Park, and Yu-Kyong Shin; project administration: Yu-Kyong Shin and Kyung-Tae Lee; supervision: Kyung-Tae Lee.

## Conflicts of interest

There are no conflicts to declare.

## Acknowledgements

This research was supported by the Medical Research Program through the National Research Foundation of Korea (NRF) funded by the Ministry of Science and ICT (NRF-2017R1A5A2014768) and the Korea Institute of Planning and Evaluation for Technology in Food, Agriculture and Forestry (IPET) through the Technology Commercialization Support Program, funded by the Ministry of Agriculture, Food and Rural Affairs (MAFRA) (RS-2024-00401688).

## References

- 1 WHO, World Obesity Atlas 2023 Obesity, <https://www.worldobesity.org/resources/resource-library/world-obesity-atlas-2023>, (accessed December 18, 2023).



- 2 A. J. M. de Leeuw, M. A. M. Oude Luttikhuis, A. C. Wellen, C. Muller and C. F. Calkhoven, Obesity and its impact on COVID-19, *J. Mol. Med.*, 2021, **99**, 899–915.
- 3 U. F. Shaik Mohamed Sayed, S. Moshawih, H. P. Goh, N. Kifli, G. Gupta, S. K. Singh, D. K. Chellappan, K. Dua, A. Hermansyah, H. L. Ser, L. C. Ming and B. H. Goh, Natural products as novel anti-obesity agents: insights into mechanisms of action and potential for therapeutic management, *Front. Pharmacol.*, 2023, **14**, 1182937.
- 4 A. Hussain, J. Lian, R. Watts, T. Gutierrez, R. Nelson, I. S. Goping and R. Lehner, Attenuation of obesity-induced hyperlipidemia reduces tumor growth, *Biochim. Biophys. Acta, Mol. Cell Biol. Lipids*, 2022, **1867**, 159124.
- 5 A. Chobot, K. Gorowska-Kowolik, M. Sokolowska and P. Jarosz-Chobot, Obesity and diabetes-Not only a simple link between two epidemics, *Diabetes/Metab. Res. Rev.*, 2018, **34**, e3042.
- 6 S. A. Polyzos, J. Kountouras and C. S. Mantzoros, Obesity and nonalcoholic fatty liver disease: From pathophysiology to therapeutics, *Metabolism*, 2019, **92**, 82–97.
- 7 V. A. Guerreiro, D. Carvalho and P. Freitas, Obesity, Adipose Tissue, and Inflammation Answered in Questions, *J. Obes.*, 2022, **2022**, 2252516.
- 8 Y. H. Lee, E. P. Mottillo and J. G. Granneman, Adipose tissue plasticity from WAT to BAT and in between, *Biochim. Biophys. Acta*, 2014, **1842**, 358–369.
- 9 U. White, Adipose tissue expansion in obesity, health, and disease, *Front. Cell Dev. Biol.*, 2023, **11**, 1188844.
- 10 D. G. Hardie, F. A. Ross and S. A. Hawley, AMPK: a nutrient and energy sensor that maintains energy homeostasis, *Nat. Rev. Mol. Cell Biol.*, 2012, **13**, 251–262.
- 11 S. Y. Lee, K. S. Chung, S. R. Son, S. Y. Lee, D. S. Jang, J. K. Lee, H. J. Kim, C. S. Na, S. H. Lee and K. T. Lee, A Botanical Mixture Consisting of *Inula japonica* and *Potentilla chinensis* Relieves Obesity via the AMPK Signaling Pathway in 3T3-L1 Adipocytes and HFD-Fed Obese Mice, *Nutrients*, 2022, **14**, 3685.
- 12 E. D. Rosen, C. J. Walkey, P. Puigserver and B. M. Spiegelman, Transcriptional regulation of adipogenesis, *Genes Dev.*, 2000, **14**, 1293–1307.
- 13 J. B. Kim, H. M. Wright, M. Wright and B. M. Spiegelman, ADD1/SREBP1 activates PPARgamma through the production of endogenous ligand, *Proc. Natl. Acad. Sci. U. S. A.*, 1998, **95**, 4333–4337.
- 14 C. Crewe, Y. Zhu, V. A. Paschoal, N. Joffin, A. L. Ghaben, R. Gordillo, D. Y. Oh, G. Liang, J. D. Horton and P. E. Scherer, SREBP-regulated adipocyte lipogenesis is dependent on substrate availability and redox modulation of mTORC1, *JCI Insight*, 2019, **5**, e129397.
- 15 M. Sekiya, N. Yahagi, T. Matsuzaka, Y. Takeuchi, Y. Nakagawa, H. Takahashi, H. Okazaki, Y. Iizuka, K. Ohashi, T. Gotoda, S. Ishibashi, R. Nagai, T. Yamazaki, T. Kadowaki, N. Yamada, J. Osuga and H. Shimano, SREBP-1-independent regulation of lipogenic gene expression in adipocytes, *J. Lipid Res.*, 2007, **48**, 1581–1591.
- 16 A. Fenzl and F. W. Kiefer, Brown adipose tissue and thermogenesis, *Horm. Mol. Biol. Clin. Invest.*, 2014, **19**, 25–37.
- 17 G. Song, H. L. Kim, Y. Jung, J. Park, J. H. Lee, K. S. Ahn, H. J. Kwak and J. Y. Um, Fruit of *Hovenia dulcis* Thunb. Induces Nonshivering Thermogenesis through Mitochondrial Biogenesis and Activation by SIRT1 in High-Fat Diet-Fed Obese Mice and Primary Cultured Brown Adipocytes, *J. Agric. Food Chem.*, 2020, **68**, 6715–6725.
- 18 L. Qiang, L. Wang, N. Kon, W. Zhao, S. Lee, Y. Zhang, M. Rosenbaum, Y. Zhao, W. Gu, S. R. Farmer and D. Accili, Brown remodeling of white adipose tissue by SirT1-dependent deacetylation of Ppargamma, *Cell*, 2012, **150**, 620–632.
- 19 Z. Wu, P. Puigserver, U. Andersson, C. Zhang, G. Adelmant, V. Mootha, A. Troy, S. Cinti, B. Lowell, R. C. Scarpulla and B. M. Spiegelman, Mechanisms controlling mitochondrial biogenesis and respiration through the thermogenic coactivator PGC-1, *Cell*, 1999, **98**, 115–124.
- 20 Q. Jiang, A. Ji, D. Li, L. Shi, M. Gao, N. Lv, Y. Zhang, R. Zhang, R. Chen, W. Chen, Y. Zheng and L. Cui, Mitochondria damage in ambient particulate matter induced cardiotoxicity: Roles of PPAR alpha/PGC-1 alpha signaling, *Environ. Pollut.*, 2021, **288**, 117792.
- 21 P. Puigserver, Z. Wu, C. W. Park, R. Graves, M. Wright and B. M. Spiegelman, A cold-inducible coactivator of nuclear receptors linked to adaptive thermogenesis, *Cell*, 1998, **92**, 829–839.
- 22 C. Contreras, R. Nogueiras, C. Dieguez, G. Medina-Gomez and M. Lopez, Hypothalamus and thermogenesis: Heating the BAT, browning the WAT, *Mol. Cell. Endocrinol.*, 2016, **438**, 107–115.
- 23 K. Ikeda and T. Yamada, UCP1 Dependent and Independent Thermogenesis in Brown and Beige Adipocytes, *Front. Endocrinol.*, 2020, **11**, 498.
- 24 R. Acin-Perez, D. L. Gatti, Y. Bai and G. Manfredi, Protein phosphorylation and prevention of cytochrome oxidase inhibition by ATP: coupled mechanisms of energy metabolism regulation, *Cell Metab.*, 2011, **13**, 712–719.
- 25 A. J. Krentz, K. Fujioka and M. Hompesch, Evolution of pharmacological obesity treatments: focus on adverse side-effect profiles, *Diabetes, Obes. Metab.*, 2016, **18**, 558–570.
- 26 R. Singh, A. Lebeda and A. Tucker, *Medicinal Plants-Nature's Pharmacy*, 2012, pp. 13–51.
- 27 A. Kijjoo and P. Sawangwong, Drugs and Cosmetics from the Sea, *Mar. Drugs*, 2004, **2**(2), 73–82.
- 28 A. Thambi and K. Chakraborty, Brown and Red Marine Macroalgae as Novel Bioresources of Promising Medicinal Properties, *J. Aquat. Food Prod. Technol.*, 2022, **31**, 227–241.
- 29 M. M. Hakim and I. C. Patel, A review on phytoconstituents of marine brown algae, *Future J. Pharm. Sci.*, 2020, **6**, 129.
- 30 S. I. Choi, H. S. Han, J. M. Kim, G. Park, Y. P. Jang, Y. K. Shin, H. S. Ahn, S. H. Lee and K. T. Lee, Eisenia bicyclis Extract Repairs UVB-Induced Skin Photoaging In Vitro and In Vivo: Photoprotective Effects, *Mar. Drugs*, 2021, **19**, 693.
- 31 S. H. Eom, D. S. Lee, Y. M. Kang, K. T. Son, Y. J. Jeon and Y. M. Kim, Application of yeast *Candida utilis* to ferment



- Eisenia bicyclis for enhanced antibacterial effect, *Appl. Biochem. Biotechnol.*, 2013, **171**, 569–582.
- 32 M. Irfan, T. H. Kwon, B. S. Yun, N. H. Park and M. H. Rhee, Eisenia bicyclis (brown alga) modulates platelet function and inhibits thrombus formation via impaired P(2)Y(12) receptor signaling pathway, *Phytomedicine*, 2018, **40**, 79–87.
- 33 H. A. Jung, S. E. Jin, B. R. Ahn, C. M. Lee and J. S. Choi, Anti-inflammatory activity of edible brown alga Eisenia bicyclis and its constituents fucosterol and phlorotannins in LPS-stimulated RAW264.7 macrophages, *Food Chem. Toxicol.*, 2013, **59**, 199–206.
- 34 B. R. Ahn, H. E. Moon, H. R. Kim, H. A. Jung and J. S. Choi, Neuroprotective effect of edible brown alga Eisenia bicyclis on amyloid beta peptide-induced toxicity in PC12 cells, *Arch. Pharmacol. Res.*, 2012, **35**, 1989–1998.
- 35 J. M. Kim, K. S. Chung, Y. S. Yoon, S. Y. Jang, S. W. Heo, G. Park, Y. P. Jang, H. S. Ahn, Y. K. Shin, S. H. Lee and K. T. Lee, Dieckol Isolated from Eisenia bicyclis Ameliorates Wrinkling and Improves Skin Hydration via MAPK/AP-1 and TGF-beta/Smad Signaling Pathways in UVB-Irradiated Hairless Mice, *Mar. Drugs*, 2022, **20**, 779.
- 36 H. S. Han, H. H. Lee, H. S. Gil, K. S. Chung, J. K. Kim, D. H. Kim, J. Yoon, E. K. Chung, J. K. Lee, W. M. Yang, Y. K. Shin, H. S. Ahn, S. H. Lee and K. T. Lee, Standardized hot water extract from the leaves of Hydrangea serrata (Thunb.) Ser. alleviates obesity via the AMPK pathway and modulation of the gut microbiota composition in high fat diet-induced obese mice, *Food Funct.*, 2021, **12**, 2672–2685.
- 37 S. W. Heo, K. S. Chung, Y. S. Yoon, S. Y. Kim, H. S. Ahn, Y. K. Shin, S. H. Lee and K. T. Lee, Standardized Ethanol Extract of Cassia mimosoides var. nomame Makino Ameliorates Obesity via Regulation of Adipogenesis and Lipogenesis in 3T3-L1 Cells and High-Fat Diet-Induced Obese Mice, *Nutrients*, 2023, **15**, 613.
- 38 Q. Q. Tang, T. C. Otto and M. D. Lane, Mitotic clonal expansion: a synchronous process required for adipogenesis, *Proc. Natl. Acad. Sci. U. S. A.*, 2003, **100**, 44–49.
- 39 L. T. Trang, N. N. Trung, D. T. Chu and N. T. H. Hanh, Percentage Body Fat is As a Good Indicator for Determining Adolescents Who Are Overweight or Obese: A Cross-Sectional Study in Vietnam, *Osong Public Health Res. Perspect.*, 2019, **10**, 108–114.
- 40 E. Fabbrini, S. Sullivan and S. Klein, Obesity and nonalcoholic fatty liver disease: biochemical, metabolic, and clinical implications, *Hepatology*, 2010, **51**, 679–689.
- 41 A. Udomkasemsab and P. Prangthip, High fat diet for induced dyslipidemia and cardiac pathological alterations in Wistar rats compared to Sprague Dawley rats, *Clin. Invest. Arterioscler.*, 2019, **31**, 56–62.
- 42 B. Chopra and A. K. Dhingra, Natural products: A lead for drug discovery and development, *Phytother. Res.*, 2021, **35**, 4660–4702.
- 43 D. B. Myung, J. H. Lee, H. S. Han, K. Y. Lee, H. S. Ahn, Y. K. Shin, E. Song, B. H. Kim, K. H. Lee, S. H. Lee and K. T. Lee, Oral Intake of Hydrangea serrata (Thunb.) Ser. Leaves Extract Improves Wrinkles, Hydration, Elasticity, Texture, and Roughness in Human Skin: A Randomized, Double-Blind, Placebo-Controlled Study, *Nutrients*, 2020, **12**, 1588.
- 44 H. Munir, L. S. C. Ward, L. Sheriff, S. Kemble, S. Nayar, F. Barone, G. B. Nash and H. M. McGettrick, Adipogenic Differentiation of Mesenchymal Stem Cells Alters Their Immunomodulatory Properties in a Tissue-Specific Manner, *Stem Cells*, 2017, **35**, 1636–1646.
- 45 S. R. Farmer, Transcriptional control of adipocyte formation, *Cell Metab.*, 2006, **4**, 263–273.
- 46 F. M. Gregoire, C. M. Smas and H. S. Sul, Understanding adipocyte differentiation, *Physiol. Rev.*, 1998, **78**, 783–809.
- 47 M. S. Madsen, R. Siersbaek, M. Boergesen, R. Nielsen and S. Mandrup, Peroxisome proliferator-activated receptor gamma and C/EBPalpha synergistically activate key metabolic adipocyte genes by assisted loading, *Mol. Cell. Biol.*, 2014, **34**, 939–954.
- 48 J. B. Kim and B. M. Spiegelman, ADD1/SREBP1 promotes adipocyte differentiation and gene expression linked to fatty acid metabolism, *Genes Dev.*, 1996, **10**, 1096–1107.
- 49 J. L. Goldstein and M. S. Brown, A century of cholesterol and coronaries: from plaques to genes to statins, *Cell*, 2015, **161**, 161–172.
- 50 I. Shimomura, H. Shimano, B. S. Korn, Y. Bashmakov and J. D. Horton, Nuclear sterol regulatory element-binding proteins activate genes responsible for the entire program of unsaturated fatty acid biosynthesis in transgenic mouse liver, *J. Biol. Chem.*, 1998, **273**, 35299–35306.
- 51 H. Shimano, N. Yahagi, M. Amemiya-Kudo, A. H. Hasty, J. Osuga, Y. Tamura, F. Shionoiri, Y. Iizuka, K. Ohashi, K. Harada, T. Gotoda, S. Ishibashi and N. Yamada, Sterol regulatory element-binding protein-1 as a key transcription factor for nutritional induction of lipogenic enzyme genes, *J. Biol. Chem.*, 1999, **274**, 35832–35839.
- 52 S. Herzig and R. J. Shaw, AMPK: guardian of metabolism and mitochondrial homeostasis, *Nat. Rev. Mol. Cell Biol.*, 2018, **19**, 121–135.
- 53 J. Cai, G. Qiong, C. Li, L. Sun, Y. Luo, S. Yuan, F. J. Gonzalez and J. Xu, Manassantin B attenuates obesity by inhibiting adipogenesis and lipogenesis in an AMPK dependent manner, *FASEB J.*, 2021, **35**, e21496.
- 54 S. W. Kang, S. I. Kang, H. S. Shin, S. A. Yoon, J. H. Kim, H. C. Ko and S. J. Kim, Sasa quelpaertensis Nakai extract and its constituent p-coumaric acid inhibit adipogenesis in 3T3-L1 cells through activation of the AMPK pathway, *Food Chem. Toxicol.*, 2013, **59**, 380–385.
- 55 C. Y. Kim, T. T. Le, C. Chen, J. X. Cheng and K. H. Kim, Curcumin inhibits adipocyte differentiation through modulation of mitotic clonal expansion, *J. Nutr. Biochem.*, 2011, **22**, 910–920.
- 56 Z. Wang, Regulation of Cell Cycle Progression by Growth Factor-Induced Cell Signaling, *Cells*, 2021, **10**, 3327.
- 57 L. Ding, J. Cao, W. Lin, H. Chen, X. Xiong, H. Ao, M. Yu, J. Lin and Q. Cui, The Roles of Cyclin-Dependent Kinases in Cell-Cycle Progression and Therapeutic Strategies in Human Breast Cancer, *Int. J. Mol. Sci.*, 2020, **21**, 1960.



- 58 J. Himms-Hagen, Brown adipose tissue thermogenesis: interdisciplinary studies, *FASEB J.*, 1990, **4**, 2890–2898.
- 59 B. Sun, M. Hayashi, M. Kudo, L. Wu, L. Qin, M. Gao and T. Liu, Madecassoside Inhibits Body Weight Gain via Modulating SIRT1-AMPK Signaling Pathway and Activating Genes Related to Thermogenesis, *Front. Endocrinol.*, 2021, **12**, 627950.
- 60 J. A. Gill and M. A. La Merrill, An emerging role for epigenetic regulation of Pgc-1alpha expression in environmentally stimulated brown adipose thermogenesis, *Environ. Epigenet.*, 2017, **3**, dxv009.
- 61 W. J. Laursen, M. Mastrotto, D. Pesta, O. H. Funk, J. B. Goodman, D. K. Merriman, N. Ingolia, G. I. Shulman, S. N. Bagriantsev and E. O. Gracheva, Neuronal UCP1 expression suggests a mechanism for local thermogenesis during hibernation, *Proc. Natl. Acad. Sci. U. S. A.*, 2015, **112**, 1607–1612.
- 62 H. A. Jung, H. J. Jung, H. Y. Jeong, H. J. Kwon, M. Y. Ali and J. S. Choi, Phlorotannins isolated from the edible brown alga *Ecklonia stolonifera* exert anti-adipogenic activity on 3T3-L1 adipocytes by downregulating C/EBPalpha and PPARgamma, *Fitoterapia*, 2014, **92**, 260–269.
- 63 T. H. Kwon, Y. X. Wu, J. S. Kim, J. H. Woo, K. T. Park, O. J. Kwon, H. J. Seo, T. Kim and N. H. Park, 6,6'-Bieckol inhibits adipocyte differentiation through downregulation of adipogenesis and lipogenesis in 3T3-L1 cells, *J. Sci. Food Agric.*, 2015, **95**, 1830–1837.
- 64 S. C. Ko, M. Lee, J. H. Lee, S. H. Lee, Y. Lim and Y. J. Jeon, Dieckol, a phlorotannin isolated from a brown seaweed, *Ecklonia cava*, inhibits adipogenesis through AMP-activated protein kinase (AMPK) activation in 3T3-L1 preadipocytes, *Environ. Toxicol. Pharmacol.*, 2013, **36**, 1253–1260.
- 65 J. Y. Park, S. E. Kang, K. S. Ahn, J. Y. Um, W. M. Yang, M. Yun and S. G. Lee, Inhibition of the PI3K-AKT-mTOR pathway suppresses the adipocyte-mediated proliferation and migration of breast cancer cells, *J. Cancer*, 2020, **11**, 2552–2559.

